

Fab	Human GPC2			Mouse GPC2		
	k_{on} (1/Ms)	k_{off} (1/s)	K_D (nM)	k_{on} (1/Ms)	k_{off} (1/s)	K_D (nM)
GPC2.D3	$9.3 \times 10^5 \pm 0.3 \times 10^5$	$0.2 \times 10^{-3} \pm 0.04 \times 10^{-3}$	0.2 ± 0.04	$1.2 \times 10^5 \pm 0.2 \times 10^5$	$0.3 \times 10^{-2} \pm 0.02 \times 10^{-2}$	22.7 ± 2.4
GPC2.D4	$8.2 \times 10^5 \pm 1.4 \times 10^5$	$2.1 \times 10^{-2} \pm 0.3 \times 10^{-2}$	25.5 ± 1.0	$6.9 \times 10^5 \pm 1.1 \times 10^5$	$10.2 \times 10^{-2} \pm 1.1 \times 10^{-2}$	155.0 ± 40.0
GPC2.D19	$2.3 \times 10^5 \pm 0.9 \times 10^5$	$2.0 \times 10^{-2} \pm 0.03 \times 10^{-2}$	11.0 ± 3.0	$0.6 \times 10^5 \pm 0.1 \times 10^5$	$0.5 \times 10^{-2} \pm 0.01 \times 10^{-2}$	77.2 ± 10.2
GPC2.D27	$11.4 \times 10^5 \pm 2.0 \times 10^5$	$1.1 \times 10^{-2} \pm 0.2 \times 10^{-2}$	9.8 ± 0.1	NB	NB	NB

F GPC2 scFv: D3, D4, 19, 27

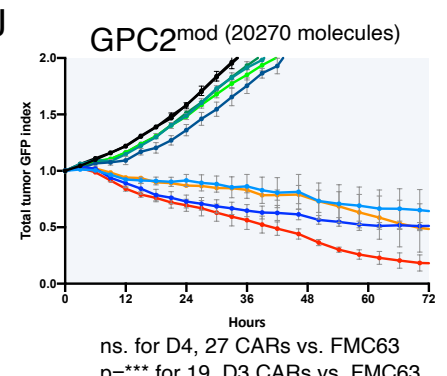
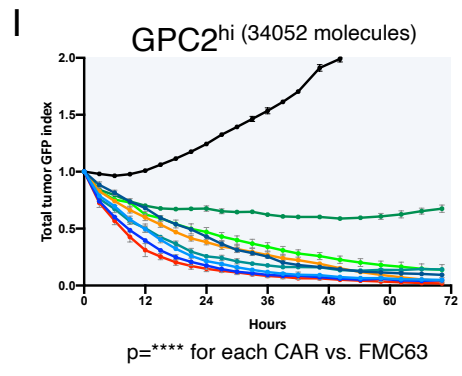
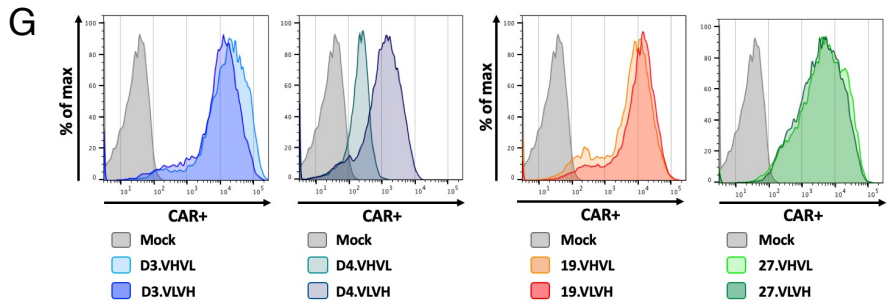
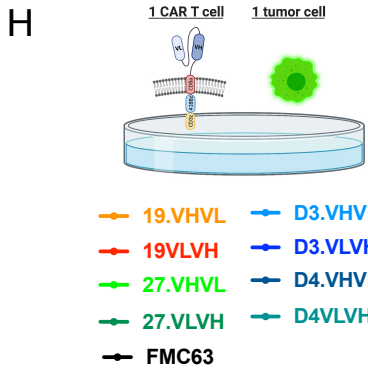
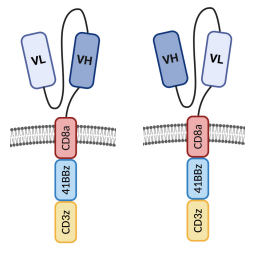


Figure S1 (related to Figure 1)

Biophysical characterization and prioritization of GPC2 binders for CAR T cell constructs

A) Summary plot representing the melting temperatures (T_m) for the four Fabs determined from the barycentric mean fluorescence. The mean (dash) is representative of duplicate measurements (dots). **B)** Summary plot representing the aggregation temperature (T_{agg}) for the four Fabs determined from static light scattering at 266 nm. The mean (dash) is representative of duplicate measurements (dots). **C)** Representative kinetic plots of Fabs GPC2.D3, GPC2.D4, GPC2.19 and GPC2.27 binding to full-length human or mouse GPC2 ectodomains. Raw data (red) was fitted using a 1:1 model (black). Binding kinetic parameters (k_{on} , k_{off} and K_D) describing the binding event are listed. Representative of two independent measurements with mean and standard error of mean (SEM). NB represents no binding. **D)** Representative kinetic plots of Fabs GPC2.D3, GPC2.D4, GPC2.19 and GPC2.27 at 250 nM concentration binding to a truncated human GPC2 core fragment (residues 24-493). **E)** Epitope binning by tandem competition assay using biolayer interferometry. Raw data is shown where the second Fab (GPC2.D3) competes with the first Fab (GPC2.19) to bind to human GPC2 immobilized on Ni-NTA biosensors. **F)** Schematic of CAR T cell constructs used for testing GPC2 scFv's. Constructs utilize CD8a hinge-transmembrane domains and 41BB costimulatory domains in variable light chain-linker-variable heavy (V_L/V_H) and variable heavy chain-linker-variable light chain (V_H/V_L) orientation **G)** representative histogram of GPC2.CAR cell surface expression among different constructs assessed by binding to fluorescently labelled recombinant GPC2 **(H)** Schematic of in vitro killing assays at 1:1 effector:target ratio. **I)** Cytolytic activity of GPC2-CAR T cells against target cell lines with supraphysiological (NGP-GPC2=GPC2^{hi}) and **J)** moderate (NBSD=GPC2^{mod}) antigen density levels in IncuCyte killing assays at 1:1 effector to target ratio. Values represent mean \pm SEM. Statistic represents two-way RM-ANOVA. Molecules/cell of GPC2 determined by QuanitBRITE PE assay are given in parenthesis. Color legend for **(I-J)** as in **(H)**. CAR T cells targeting CD19 (FMC63) were used as negative control (black).

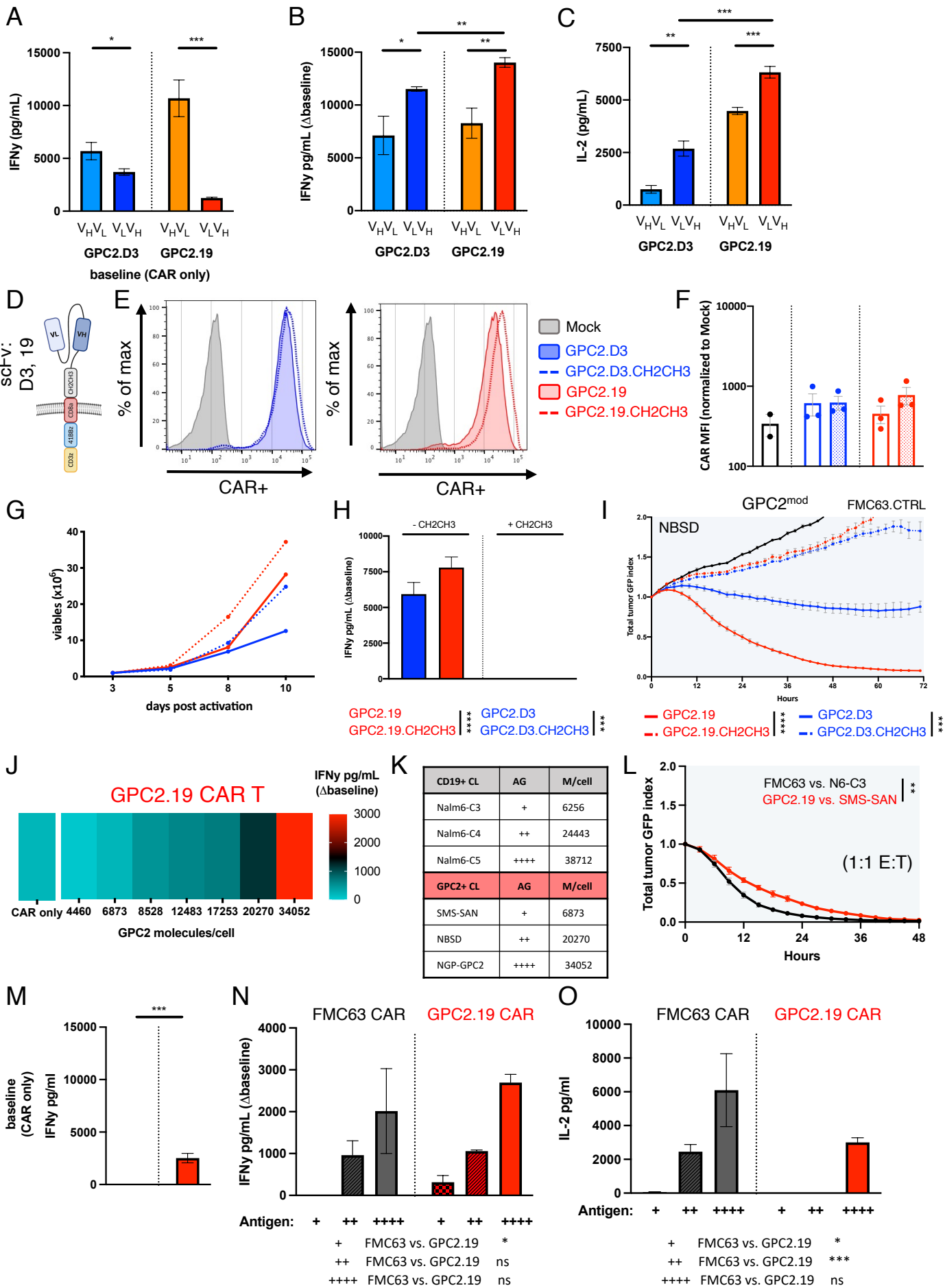


Figure S2 (Related to Figure 1).

Orientation of GPC2 targeted scFvs and extracellular spacer length for maximum efficacy in CAR T cell constructs

A) Baseline levels of IFN γ in GPC2-CAR T cell constructs utilizing scFv-19 or scFv-D3 in V_HV_L and V_LV_H orientations **B)** Secretion of IFN γ (Δ baseline) and **C)** IL-2 of GPC2.D3 and GPC2.19 CAR T-cell constructs in V_HV_L and V_LV_H orientations in response to transgenic overexpression of antigen (NGP-GPC2 =GPC2^{hi}) in 24hr co-culture assays (mean \pm SD). Representative of n=3 independent experiments with 3 individual DNRs. Statistic represents student's t-test (**** = p<0.0001, *** = p<0.001, ** = p<0.01, * = p<0.05), ns = p > 0.05). **D)** Schematic of GPC2-CAR T cells constructs incorporating an extracellular CH2CH3 spacer domain **E)** representative histogram of GPC2.D3.8TM.41BBz and GPC2.19.8TM.41BBz CAR cell surface expression of constructs with/without CH2CH3 spacer domain. **F)** Mean fluorescent intensity of GPC2-CAR cell surface expression across experiments (log10 of CAR MFI normalized for Mock, day 10 or 11, n=3 independent experiments with 3 different donors, mean \pm SEM). Color legend for **(E-I)** as in **(D)**. One-way multiple comparisons ANOVA = ns for all conditions. **G)** Expansion of GPC2.D3.8TM.41BBz and GPC2.19.8TM.41BBz CAR T cells with/without CH2CH3 spacer domain shown as total viable cells (x10⁶ cells) during in vitro culture (representative of n=3 independent experiments with 3 different donors). **H)** IFN γ production of GPC2.D3.8TM.41BBz and GPC2.19.8TM.41BBz CAR T cells with/without CH2CH3 spacer domain in response to 24hr co-culture with NBSD (GPC2^{mod}). Values represent mean \pm SD, representative of n=3 independent experiments with n=3 individual DNRs. Statistic represents student's t-test. **I)** Cytolytic activity of GPC2-CAR T cells with/without CH2CH3 spacer domain in killing assays at 1:1 effector:target ratio against NBSD (GPC2^{mod}) cell lines. Values represent mean \pm SD, representative of n=3 independent experiments with n=3 individual DNRs. Statistical test in represents two-way RM-ANOVA (**** = p<0.0001, *** = p<0.001). **J)** Heatmap depicting baseline levels of IFN γ and secretion of IFN γ (Δ baseline) by GPC2.19 CAR T cells in response to cell lines with varying antigen levels. Representative of n=3 independent experiments. **K)** Quantitative antigen density (molecules/cell) of CD19 on Nalm6 clonal cell lines and GPC2 on NB cell lines assessed by QuantiBrite PE assay used for side-by-side comparative experiments in (L-N). **L)** Cytolytic activity in antigen^{lo} killing assays of CD19-CAR T cells (FMC63) against Nalm6 clone 3 and GPC2.19 CAR T cells against SMS-SAN at 1:1 effector:target ratio. Both CAR constructs utilize the same 8TM.41BBz architecture. Values represent mean \pm SD, representative of n=3 independent experiments with n=3 individual DNRs. Statistical test in represents two-way RM-ANOVA (**= p<0.01). **M)** Baseline levels of IFN γ in CD19-CAR T cells (FMC63) and GPC2.19 CAR T cells in the absence of antigen and **N)** Secretion of IFN γ (Δ baseline) and **O)** IL2 against respective antigen^{lo}, antigen^{med} and antigen^{hi} target cell lines indicated in (K) in response to 24hr co-culture. Values represent mean \pm SD, representative of n=3 independent experiments with n=3 individual DNRs. Statistic represents student's t-test.

A

Stanford University	PT_ID	Sample TP	Diagnosis	MYCN status	M/F	Age at Sample TP
	ST16	diagnosis	HR-NBL	<i>MYCN</i> ampl.	male	2 yrs 9 mo
	ST16R	relapse				2 yrs 11 mo
	ST36	diagnosis	HR-NBL	Neg.	female	2 yrs 10 mo
	ST77	diagnosis	HR-NBL	Neg.	male	7 yrs 5 mo
	ST5	relapse	Composite PCC	Neg.	female	6 yrs 1 mo
St. Anna's CCRI	PT_ID	Sample TP	Diagnosis	MYCN status	M/F	Age at Sample TP
	AT1	diagnosis	HR-NBL	<i>MYCN</i> ampl.	female	1 yrs 9 mo
	AT2	diagnosis	HR-NBL	Neg.	male	7 yrs
	AT3	diagnosis	HR-NBL	<i>MYCN</i> ampl.	male	2 yrs 5 mo
	AT4	diagnosis	HR-NBL	<i>MYCN</i> ampl.	female	7 yrs 2 mo

B

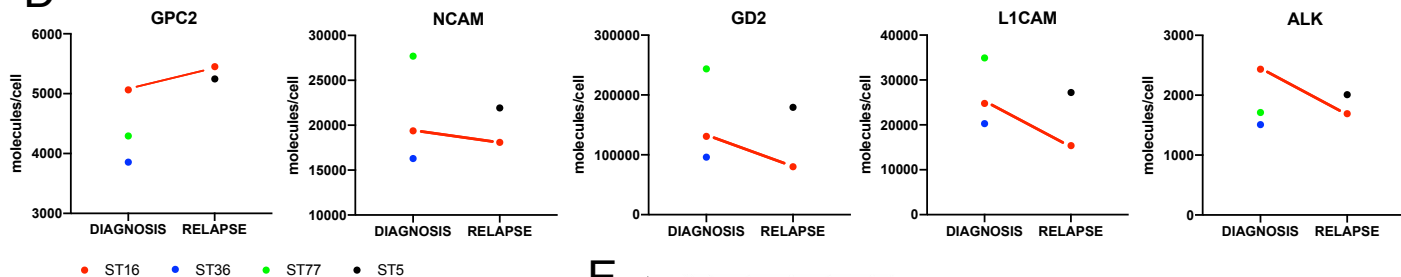
Group	GPC2			NCAM		
	CL	BM_TU	PDX	CL	BM_TU	PDX
N=	11	9	15	11	9	15
AVE	8924	4262	9479	43994	21885	52269
SEM	1843	469	1358	8732	1961	2172
MIN	2898	1425	3458	3110	14435	38425
MAX	21312	6041	18637	96562	31698	67108

Group	GD2			L1CAM			ALK			B7H3		
	CL	BM_TU	PDX	CL	BM_TU	PDX	CL	BM_TU	PDX	CL	BM_TU	PDX
N=	11	9	15	11	9	15	11	9	15	11	4	15
AVE	277564	301763	400201	41242	21209	41889	2239	2300	6920	18488	3156	25382
SEM	69227	75046	47816	8188	2392	2377	236	558	827	3649	618	3869
MIN	49583	80096	9307	5354	10944	19419	1509	1383	2407	2895	2018	4980
MAX	700904	683695	722189	103491	34908	54194	2434	6683	12443	44414	4031	65206

C

	GPC2	NCAM	L1CAM	ALK	B7-H3
GD2	****	****	****	****	***
GPC2		ns	ns	ns	ns
NCAM			ns	ns	ns
L1CAM				ns	ns
ALK					ns

D



E

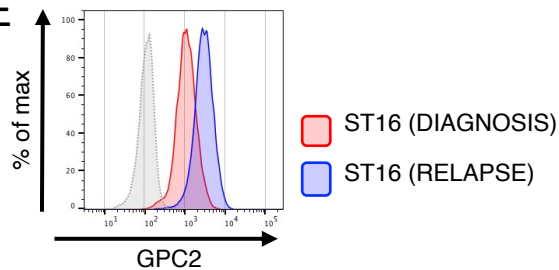
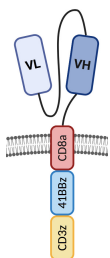


Figure S3 (Related to Figure 2).

Patient Characteristics of clinical samples of neuroblastoma cells metastatic to the bone marrow

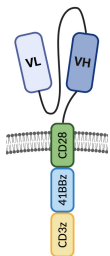
A) Patient characteristics including Patient ID, sample timepoint, diagnosis, MYCN status, male/female, age and institution at which sample was collected and analyzed of bone-marrow infiltrating neuroblastoma tumor samples utilized for multicolor antigen density quantification assay. **B)** Sample parameters (sample size, molecules/cell average, standard error of the mean and minimum/maximum values of data shown in Figure 2D. **C)** Statistical comparison of antigen density on bone-marrow infiltrating neuroblastoma cells using one-way multiple comparison ANOVA (**** = $p < 0.0001$). **D)** Molecules/Cell of GPC2, NCAM, GD2, L1CAM and ALK measured in 3 primary and 2 relapsed samples from neuroblastoma patients derived from the Stanford Pediatric Bass Center Tissue bank. Red line binds diagnostic vs relapsed paired samples patient ST16. **E)** Cell surface expression of GPC2 in patient-derived cell lines from matched diagnostic and relapsed ST16 sample shown in **(E)**.

Table S1 (Related to Figure 3). Protein sequences of CAR constructs



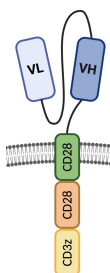
GPC2.19VLVH.8aTM.41BBz

MLLVTSLLLCELPHPAFLIPDIQMTQSPSSLSASIGDRVITTCQASQDISDYLNWYQQKPGKAPKLLIYDASNLETGVPSRF
SGSGSGTDFFTTISSLQPEDVATYYCQYDNLPIITFGQGTKLEIKRGGGGSGGGASGGGGSQLLQESGPGLVKPSSETLSLT
CTVSGGSISSSSYYWSWIRQPPGKLEWIGSIYSGSTYYNPSLKSRTISVDTSKNQFSLKSSVTAADTAVYYCARRVSGH
PFDPWGQGLTAVSSATTPAPRPPTAPTASQPLSLRPEACRPAAGGAVHTRGLDFACDIYWAPLAGTCGVLLLSLVITL
YCKRGRKLLYIFKQPFMRPVQTTQEEDGCSCRFPEEEEGGCELRVKFSRSADAPAYKQGQNQLYNELNLGRREEYDVLK
RRGRDPPEMGGKPRRKNPQEGLYNELQDKMAEAYSEIGMKGERRRGKGGHDGLYQGLSTATKDTYDALHMQALPPR



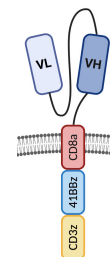
GPC2.19VLVH.28TM.41BBz

MLLVTSLLLCELPHPAFLIPDIQMTQSPSSLSASIGDRVITTCQASQDISDYLNWYQQKPGKAPKLLIYDASNLETGVPSRF
SGSGSGTDFFTTISSLQPEDVATYYCQYDNLPIITFGQGTKLEIKRGGGGSGGGASGGGGSQLLQESGPGLVKPSSETLSLT
CTVSGGSISSSSYYWSWIRQPPGKLEWIGSIYSGSTYYNPSLKSRTISVDTSKNQFSLKSSVTAADTAVYYCARRVSGH
PFDPWGQGLTAVSSAAAIEVMYPPPYLDNEKSNGTIIHVKGKHLCPSPFPGPSKPFVWLVVGGVLACYSLLVTVAFIIF
WVKRGRKLLYIFKQPFMRPVQTTQEEDGCSCRFPEEEEGGCELRVKFSRSADAPAYKQGQNQLYNELNLGRREEYDVLK
KRRGRDPPEMGGKPRRKNPQEGLYNELQDKMAEAYSEIGMKGERRRGKGGHDGLYQGLSTATKDTYDALHMQALPPR



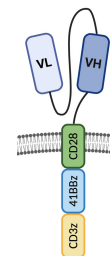
GPC2.19VLVH.28TM.28z

MLLVTSLLLCELPHPAFLIPDIQMTQSPSSLSASIGDRVITTCQASQDISDYLNWYQQKPGKAPKLLIYDASNLETGVPSRF
SGSGSGTDFFTTISSLQPEDVATYYCQYDNLPIITFGQGTKLEIKRGGGGSGGGASGGGGSQLLQESGPGLVKPSSETLSLT
CTVSGGSISSSSYYWSWIRQPPGKLEWIGSIYSGSTYYNPSLKSRTISVDTSKNQFSLKSSVTAADTAVYYCARRVSGH
PFDPWGQGLTAVSSAAAIEVMYPPPYLDNEKSNGTIIHVKGKHLCPSPFPGPSKPFVWLVVGGVLACYSLLVTVAFIIF
WVRSKRSLHSDYMNMTPRRPGPTRKHYPYAPPRDFAAYRSRVKFSRSADAPAYKQGQNQLYNELNLGRREEYDVL
DKRRGRDPPEMGGKPRRKNPQEGLYNELQDKMAEAYSEIGMKGERRRGKGGHDGLYQGLSTATKDTYDALHMQALPPR



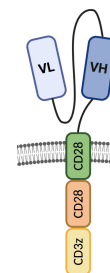
GPC2.D3VLVH.8aTM.41BBz

MLLVTSLLLCELPHPAFLIPDIQMTQSPSTLSAFVGDRVITTCRASQSISSWLAWYQQKPGKAPKLLIYAASLTQSGVPSRF
SGSGSGTEFTTISSLQPEDFATYYCQQLNSYPITFGQGTREIKRGGGGSGGGGSEVQLVETGGGVVVKPGGSLRLS
CAASGFTFSDYYMSWIRQAPGKLEWVSYISSSGSTIYADSVKGRFTISRDNKNTLYLQMNSLRAEDTAVYYCARESGYD
YFDYWGGQGLTAVSSATTPAPRPPTAPTASQPLSLRPEACRPAAGGAVHTRGLDFACDIYWAPLAGTCGVLLLSLVIT
LYCKRGRKLLYIFKQPFMRPVQTTQEEDGCSCRFPEEEEGGCELRVKFSRSADAPAYKQGQNQLYNELNLGRREEYDVLK
KRRGRDPPEMGGKPRRKNPQEGLYNELQDKMAEAYSEIGMKGERRRGKGGHDGLYQGLSTATKDTYDALHMQALPPR



GPC2.D3VLVH.28TM.41BBz

MLLVTSLLLCELPHPAFLIPDIQMTQSPSTLSAFVGDRVITTCRASQSISSWLAWYQQKPGKAPKLLIYAASLTQSGVPSRF
SGSGSGTEFTTISSLQPEDFATYYCQQLNSYPITFGQGTREIKRGGGGSGGGGSEVQLVETGGGVVVKPGGSLRLS
CAASGFTFSDYYMSWIRQAPGKLEWVSYISSSGSTIYADSVKGRFTISRDNKNTLYLQMNSLRAEDTAVYYCARESGYD
YFDYWGGQGLTAVSSAAAIEVMYPPPYLDNEKSNGTIIHVKGKHLCPSPFPGPSKPFVWLVVGGVLACYSLLVTVAFIIF
WVKRGRKLLYIFKQPFMRPVQTTQEEDGCSCRFPEEEEGGCELRVKFSRSADAPAYKQGQNQLYNELNLGRREEYDVLK
KRRGRDPPEMGGKPRRKNPQEGLYNELQDKMAEAYSEIGMKGERRRGKGGHDGLYQGLSTATKDTYDALHMQALPPR



GPC2.D3VLVH.28TM.28z

MLLVTSLLLCELPHPAFLIPDIQMTQSPSTLSAFVGDRVITTCRASQSISSWLAWYQQKPGKAPKLLIYAASLTQSGVPSRF
SGSGSGTEFTTISSLQPEDFATYYCQQLNSYPITFGQGTREIKRGGGGSGGGGSEVQLVETGGGVVVKPGGSLRLS
CAASGFTFSDYYMSWIRQAPGKLEWVSYISSSGSTIYADSVKGRFTISRDNKNTLYLQMNSLRAEDTAVYYCARESGYD
YFDYWGGQGLTAVSSAAAIEVMYPPPYLDNEKSNGTIIHVKGKHLCPSPFPGPSKPFVWLVVGGVLACYSLLVTVAFIIF
WVRSKRSLHSDYMNMTPRRPGPTRKHYPYAPPRDFAAYRSRVKFSRSADAPAYKQGQNQLYNELNLGRREEYDVL
DKRRGRDPPEMGGKPRRKNPQEGLYNELQDKMAEAYSEIGMKGERRRGKGGHDGLYQGLSTATKDTYDALHMQALPPR

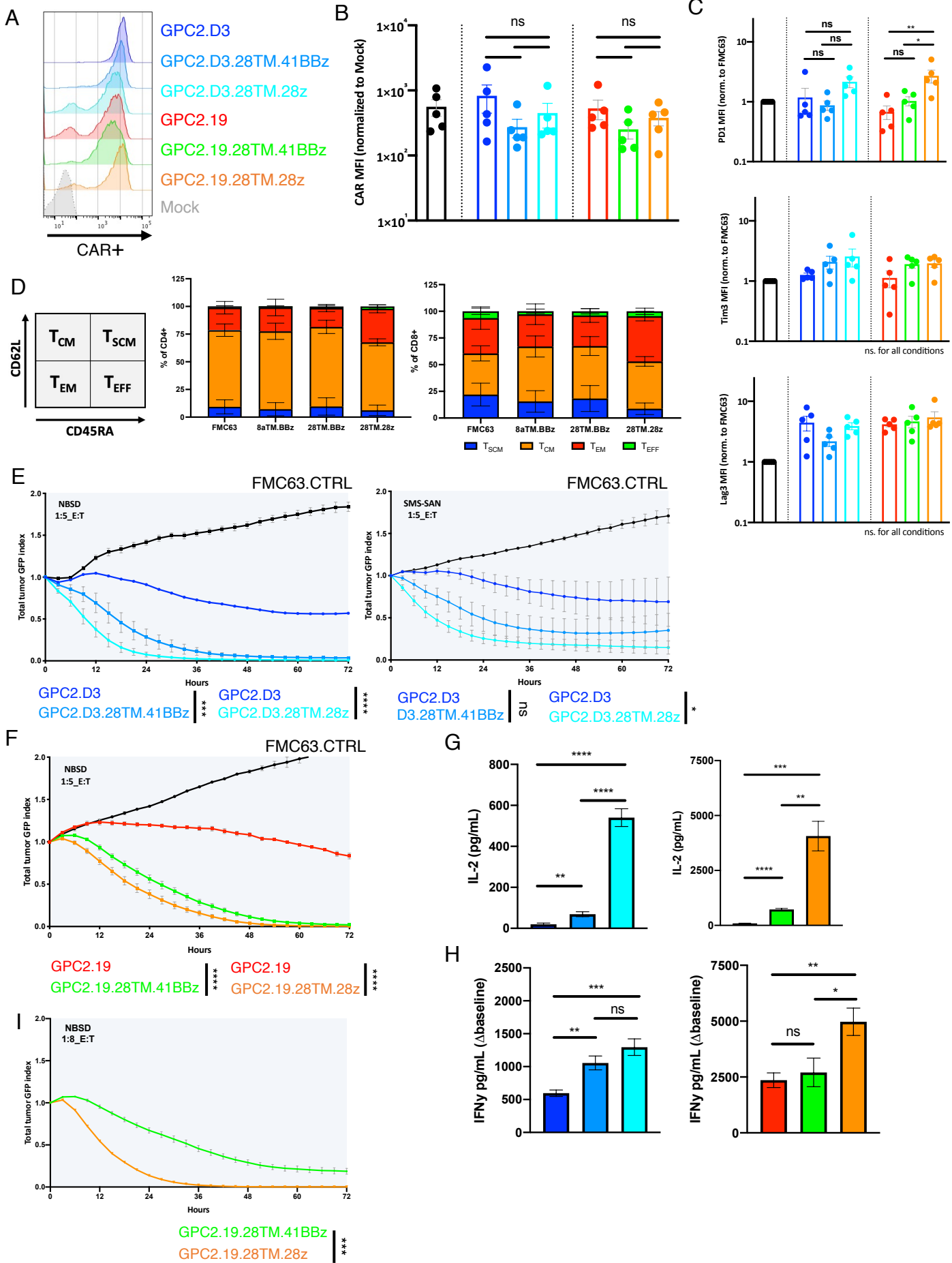


Figure S4 (Related to Figure 3).

Incorporation of CD28 TM \pm CD28 costimulatory endodomain renders GPC2 CAR T cells efficacious against GPC2^{mod} and GPC2^{lo} neuroblastomas

A) Representative histogram of GPC2-CAR cell surface expression among different constructs assessed by binding to fluorescently labelled recombinant GPC2. **B)** Mean fluorescent intensity of CAR expression in all GPC2-CAR constructs and FMC63.CTRL CAR T cells (shown in black). Data represents log₁₀ of CAR MFI normalized to Mock, day 10 or 11, n=5 independent experiments with 5 different donors, mean \pm SEM. One-way multiple comparisons ANOVA = ns for all conditions. **C)** Exhaustion marker profile of all CAR T cell constructs evaluated by flow cytometry, Mean fluorescent intensity of PD1, Tim3, Lag3 expression. Data represents log₁₀ of MFI normalized to FMC63.CTRL CAR (shown in black), day 10 or 11, n=5 independent experiments with 5 different donors, mean \pm SEM). Statistics represent one-way multiple comparisons ANOVA. **D)** Phenotypic analysis of control FMC63 CAR T cells and different GPC2.19 CAR T cells showing the frequency of stem cell memory, central memory, effector memory and effector T-cells defined by CD45RA and CD62L surface expression. Analyzed on day 10, n=5 independent experiments with 5 different donors. Values represent mean \pm SEM, one-way multiple comparisons ANOVA = ns for all conditions. **E)** Cytolytic activity of GPC2.D3 CAR T-cells incorporating CD28 TM domains with 41BB or CD28 costimulatory domains when challenged with 5x excess tumor of SMS-SAN (GPC2^{lo}) or NBSD (GPC2^{mod}) or **F)** respective variations of GPC2.19 CAR T-cells when challenged with 5x excess tumor of NBSD (GPC2^{mod}) in comparison to 8TM.41BBz constructs and FMC63 control CAR T cells. Values represent mean \pm SEM, representative of n=3 independent experiments with n=3 individual DNRs. **G)** IL2 secretion and **H)** IFN γ secretion of the different GPC2.D3 CAR T-cells and GPC2.19 CAR T-cell constructs assessed in comparison to original constructs harboring CD8 TM domains in response to 24hr co-culture with NBSD (GPC2^{mod}) cell lines. Values represent mean \pm SD, representative of n=3 independent experiments with n=3 individual DNRs. Statistic represents Student's t-test. Color legend for **(B, C, D)** as in **(A)**. **I)** Cytolytic activity of GPC2.19 CAR T cells incorporating CD28 TM domains with 41BB or CD28 costimulatory domains when challenged with 8x excess tumor of NBSD (GPC2^{mod}). Values represent mean \pm SEM, representative of n=3 independent experiments with n=3 individual DNRs. Statistical test in **(E, F, I)** represents two-way RM-ANOVA (**** = p<0.0001, *** = p<0.001, ** = p<0.01, * = p<0.05), ns = p > 0.05).

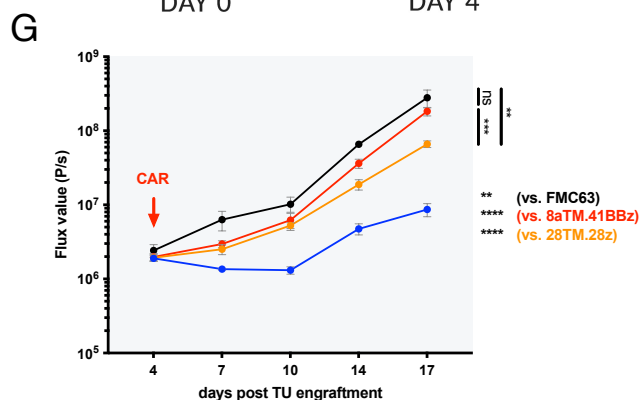
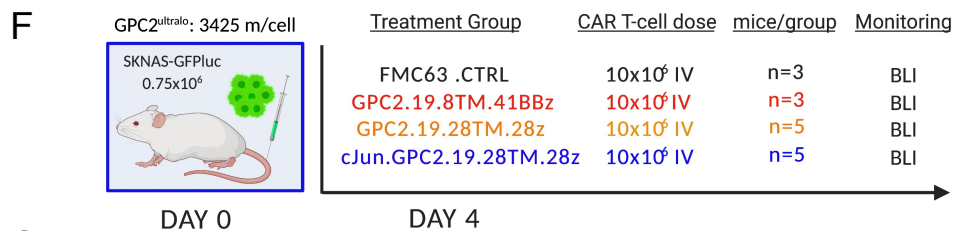
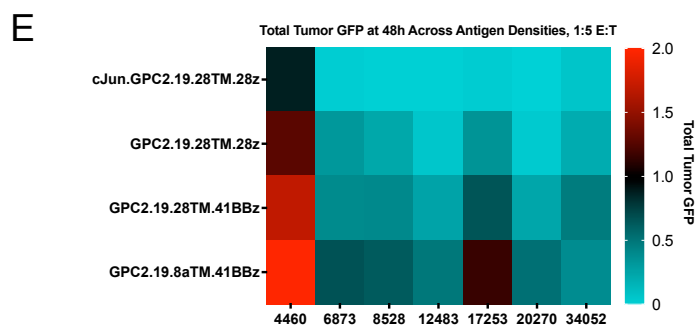
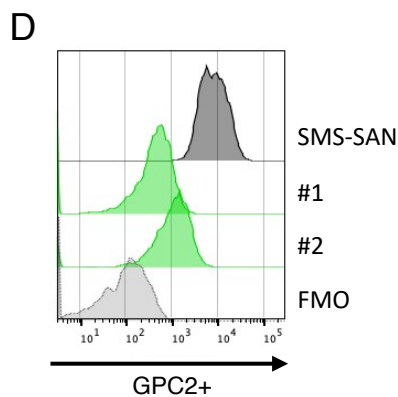
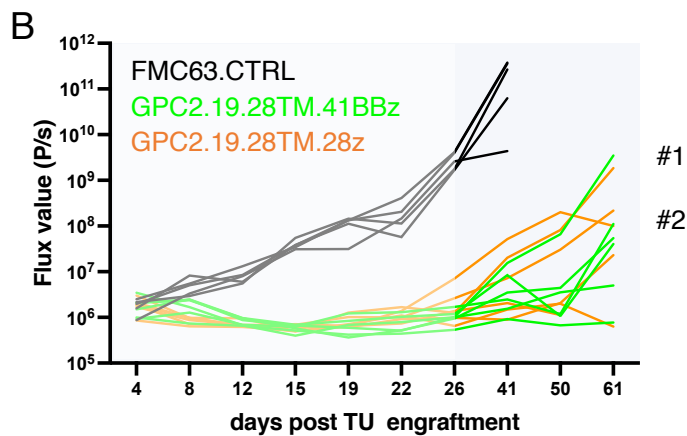
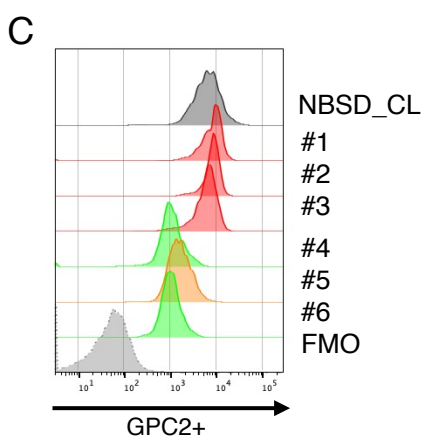
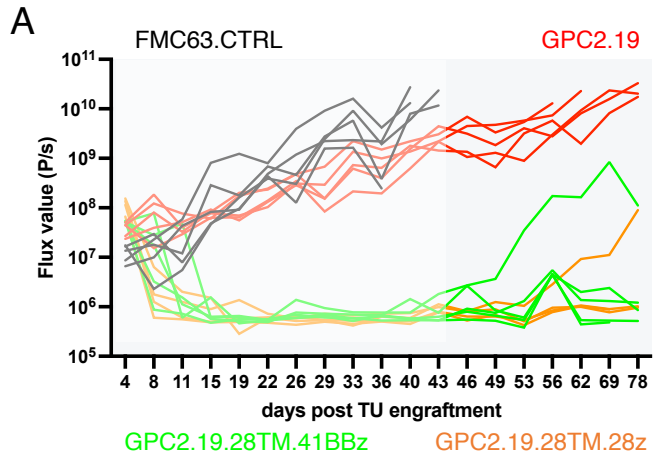
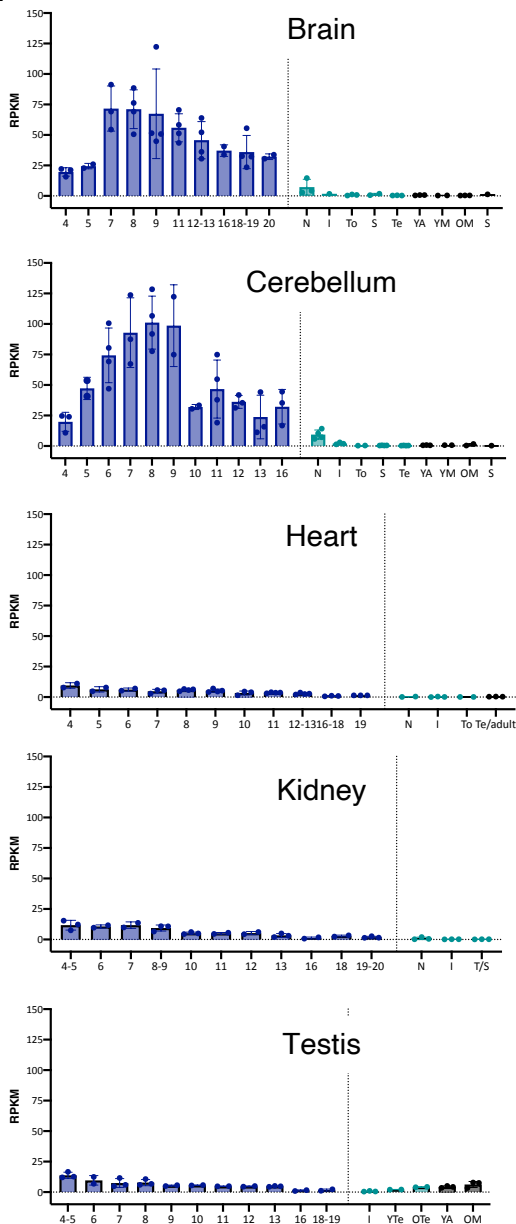


Figure S5 (Related to Figure 5 and 6).

Late Relapse is Associated with Emergence of GPC2^{ultra} recurrence and can be addressed by c-JUN Overexpression in GPC2.28TM.28z-CAR T cells

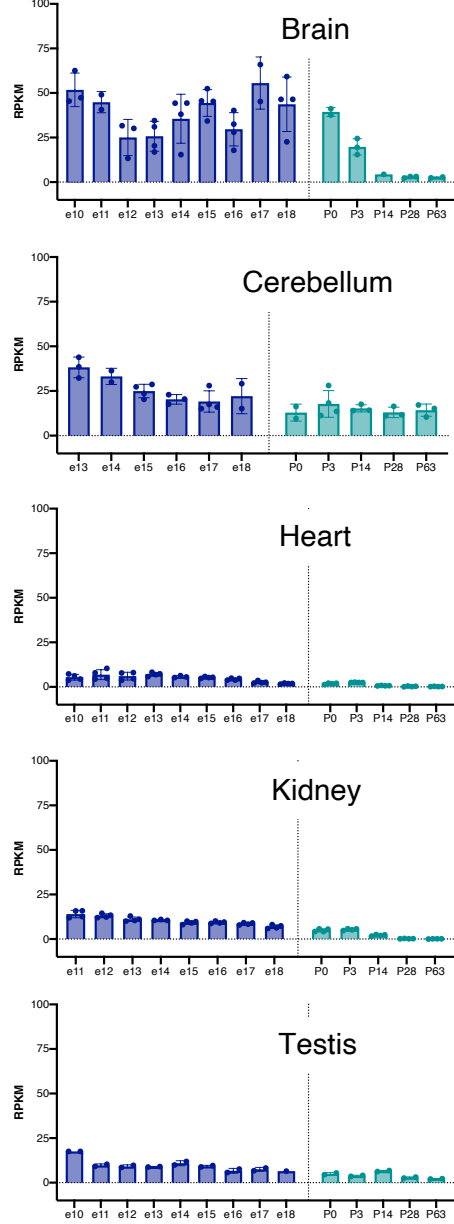
A) Long-term assessment of tumor burden (FLUX [P/s] values) assessed by IVIS imaging of experiment shown in Figure 3D-G. **B)** Long-term assessment of tumor burden (FLUX [P/s] values) assessed by IVIS imaging of experiment shown in Figure 3H-K. **C)** Flow Cytometric analysis of GPC2 antigen density in para-orthotopic tumors at endpoint shown in (A), treated with GPC2.19 CAR T cells containing CD8 TM and 41BB co-stimulatory domains (modest anti-tumor response, marked in red) in comparison to recurring tumors post complete response after treatment with GPC2.19.28TM.41BBz (marked in green) or GPC2.19.28TM.28z CAR T cells (marked in orange). FMO = fluorescent minus one control sample. NBSD control sample (grey histogram) represents cell line grown *in vitro*. **D)** Flow cytometric analysis of GPC2 antigen density in metastatic liver tumors at endpoint shown in (B), color code as in C. SMS-SAN control represents cell line post metastatic engraftment in untreated NSG mouse. **E)** Heatmap depicting killing capacity of all GPC2.19 CAR T cell constructs post 48hrs of co-culture in response to cell lines with varying antigen levels of GPC2 at 1:5 effector to target ratio. Representative of n=3 independent experiments. **F)** Schematic of *in vivo* experimental setup testing GPC2.19-CAR T cell constructs or FMC63.CTRL in metastatic neuroblastoma model post IV injection of 0.75×10^6 GPC2^{ultra} tumor cells (SKNAS: 3425m/cell). Mice were treated on Day 4 via IV tail vein injection with 10×10^6 CAR T cells **G)** FLUX [P/s] values of tumor burden assessed by IVIS imaging (color legend as in A). Values represent mean \pm SEM. Statistical test represents two-way RM-ANOVA (**** = $p < 0.0001$, *** = $p < 0.001$, ** = $p < 0.01$, * = $p < 0.05$), ns = $p > 0.05$).

A Human GPC2 (ENSG00000213420)



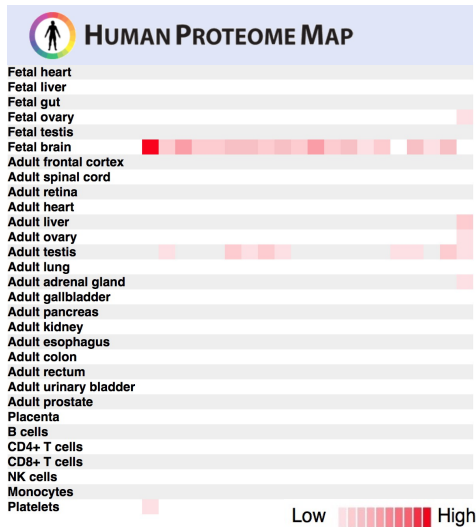
- prenatal (weeks post-conception)
- pediatric (N_newborn, I_infant, To_toddler, S_school, Te_teenager)
- adult (YA_young adult, YM_young mid-age, OM_older midage, S_senior)

B Murine GPC2 (ENSMUSG00000029510)



- prenatal
- postnatal

C



D

Prenatal Murine Brain

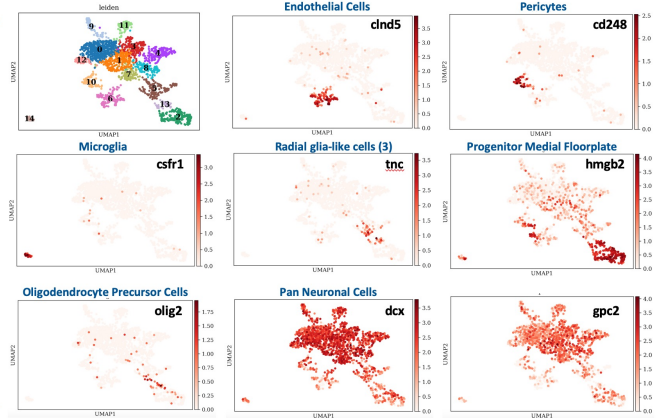
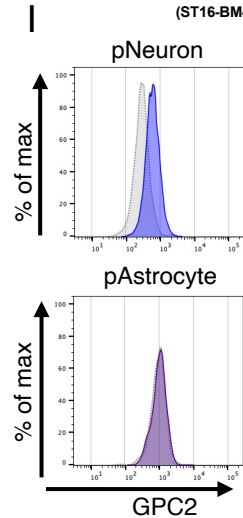
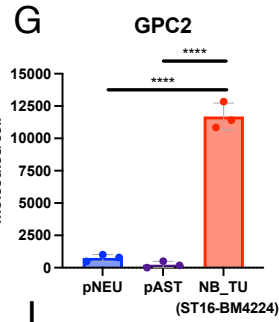
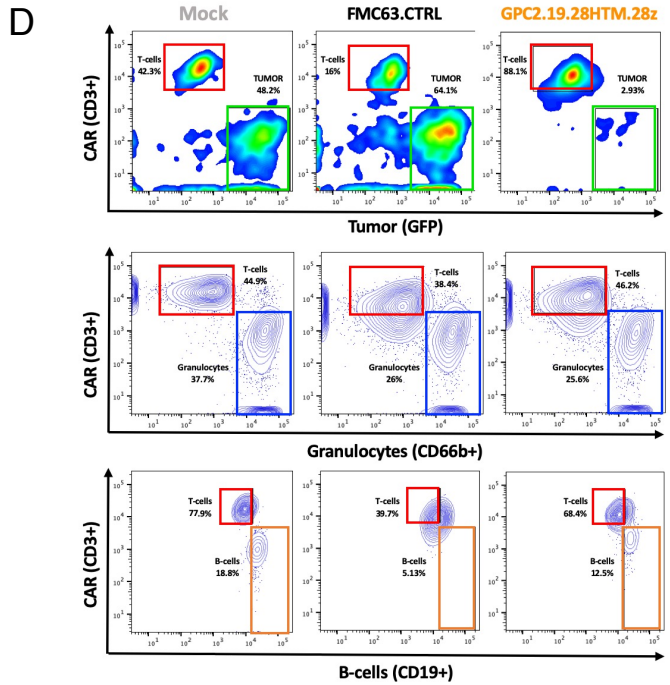
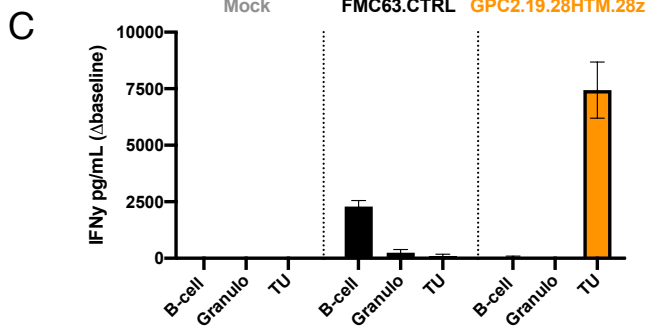
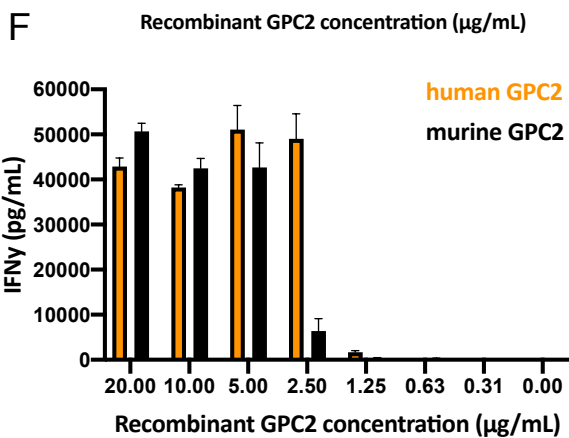
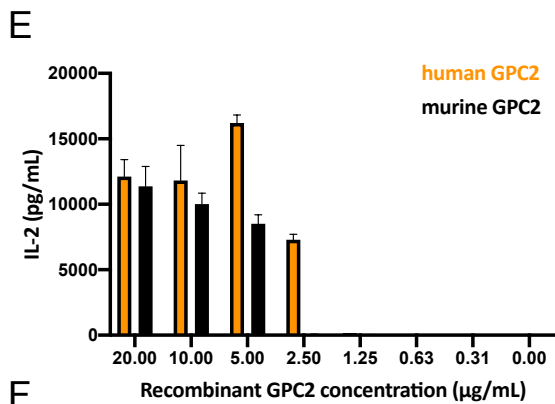
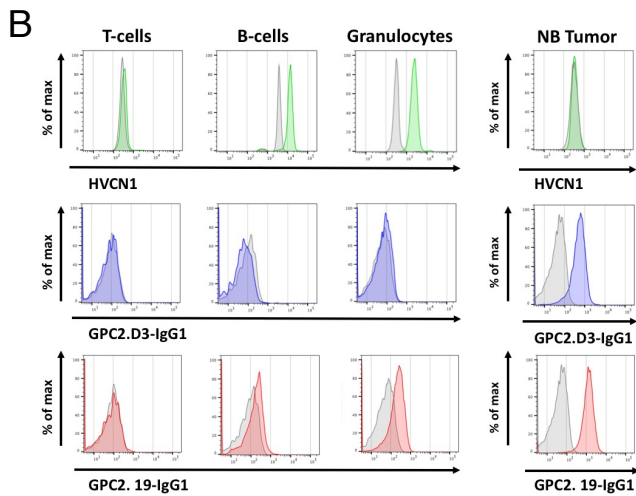
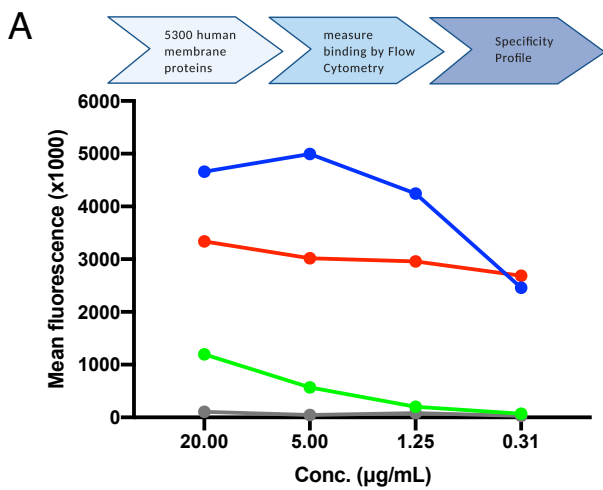


Figure S6 (Related to Figure 7).

Pattern of GPC2 expression restricted to fetal brain is similar between murine and human tissues

A) Gene expression of *GPC2* in organs across human tissue developmental stages and **B)** murine developmental stages sourced from <https://apps.kaessmannlab.org/evodevoapp/> (Cardoso-Moreira et. al 2019). Values represent RPKM, mean \pm SD **C)** Protein expression of GPC2 across normal human tissues assessed by Mass Spectrometry sourced from the Human Proteome Map (www.humanproteomemap.org). **D)** UMAP projections showing distinct cell populations from single-cell RNA-sequencing data in fetal, murine ventral midbrain. Data sourced via GEO accession GSE76381 (La Manno et. al, Cell 2016), colored by cluster and according to **E)** UMAP projection of single cells RNA-sequencing data, colored by expression of the indicated genes, which mark various populations in the brain. Note that GPC2 is highly expressed in the pan-neuronal population, as marked by DCX. Color indicates log-transformed, depth-normalized counts per cell.



H

Group	pNEU	pAST	ST16-BM4224
AVE	761	232	11698
SEM	150	149	597
MIN	487	0	10843
MAX	1005	511	12848

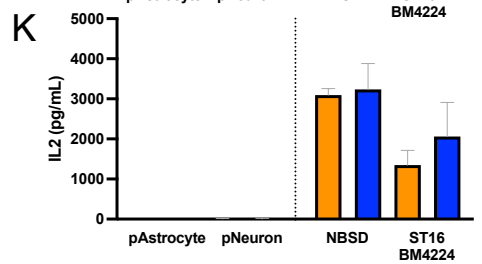
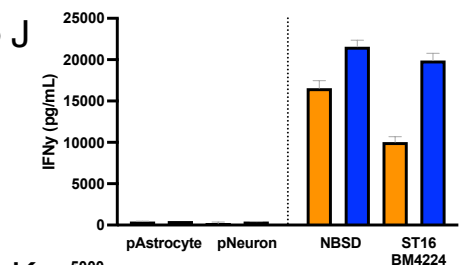


Figure S7 (Related to Figure 8).

GPC2 CAR T cells recognize human and murine GPC2 in a specific manner

A) Membrane Protein Array screen of >5300 proteins to test for off-target binding of GPC2.19-IgG1 antibody. Mean fluorescence indicates binding by flow cytometry at increasing antibody concentrations against positive control (Protein A), negative control (vector), GPC2 and HVCN1. **B)** Flow cytometric analysis of expression of HVCN1 on T cells (negative control), B-cells and granulocytes and assessment of cross-reactive binding of GPC2.19-IgG1 and GPC2.D3-IgG1 in comparison to binding of neuroblastoma tumor cells (NBSD cell line). Grey histograms represent respective isotype control. **C)** IFN γ secretion of GPC2.19.28TM.28z and FMC63.41BBz CAR T cells in response to 24hr co-culture with autologous B-cells and granulocytes or NBSD neuroblastoma tumor cells as measured by ELISA (values represent mean \pm SD) and **D)** Cytotoxicity after 24hrs co-culture at 1:1 ratio and as assessed by flow cytometry. Representative of n=4 experiments with n=4 donors for B-D. **E)** Secretion of IFN γ and **F)** IL2 of GPC2.19.28TM.28z CAR T cells after 24hrs coculture with plate-bound recombinant human or murine GPC2 at increasing concentrations (μ g/mL). Representative of n=3 independent experiments with n=3 different donors. Values shown as mean \pm SD. **G)** Quantification of molecules/cell of GPC2 on primary human Astrocytes and Neurons in comparison to patient-derived NB tumor cells isolated from the bone marrow at relapse (ST16-BM4224). Combined data from n=3 independent experiments. Statistic represents Student's t-test (***) = p<0.001). **H)** Corresponding sample parameters (average, standard error of the mean and minimum/maximum values) of data shown in **(G)**. **I)** Representative Flow Cytometry plots of GPC2 staining on primary Neurons and Astrocytes quantified in **(G)**. **J)** Cytokine levels of IFN γ (no CAR only baseline detected) and **K)** IL2 secreted by GPC2.19.28TM.28z and cJUN.GPC2.19.28TM.28z post 24hrs of co-culture with primary neurons and astrocytes in comparison to the NB cell line NBSD and NB tumor cells isolated from the bone marrow at relapse (ST16-BM4224). Representative of experiment with n=4 DNRs (mean \pm SD).

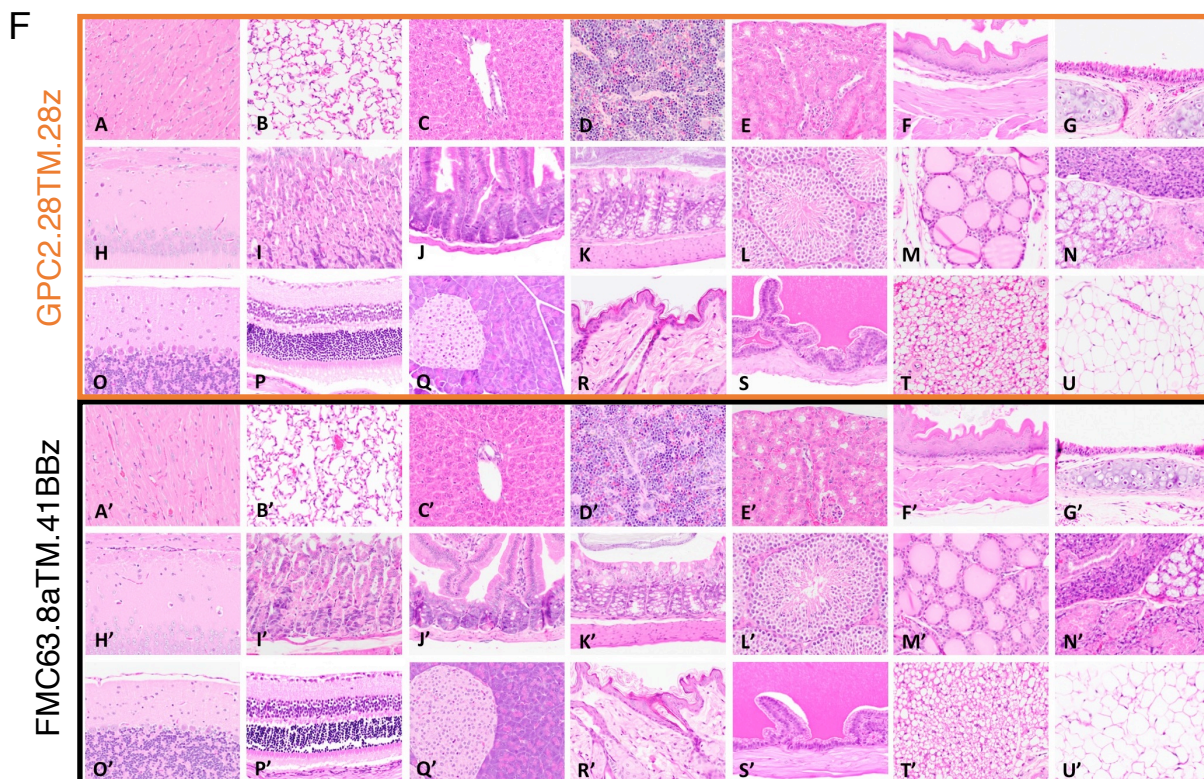
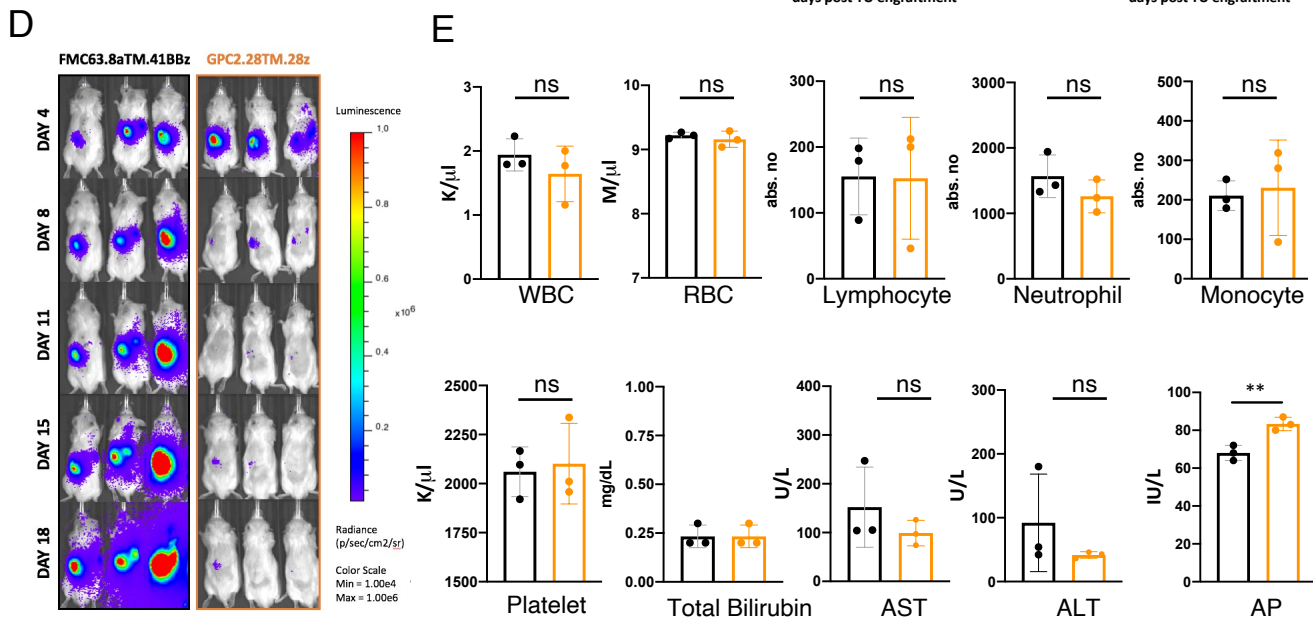
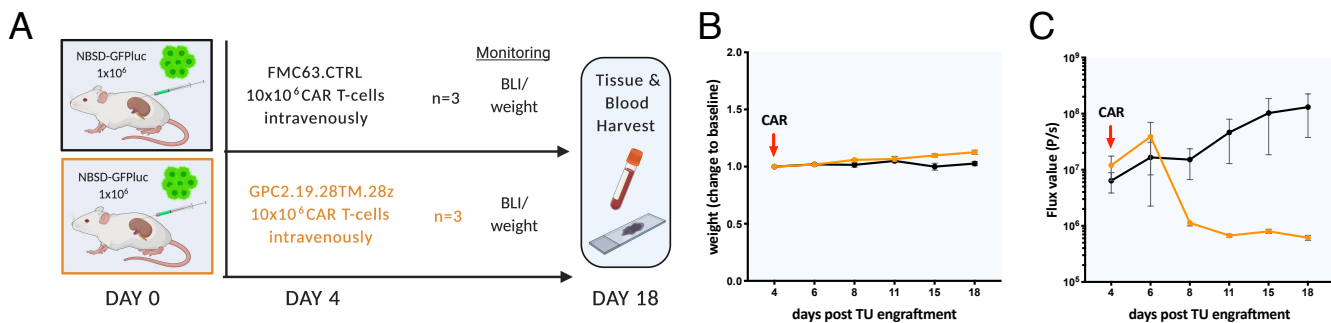


Figure S8 (Related to Figure 8).

GPC2 CAR T-cells eradicate tumor in the absence of toxicity

A) Schematic of experimental setup (n=1): NSG mice were engrafted with 1×10^6 NBSD tumor cells beneath the left renal capsule and treated with 10×10^6 GPC2.19.28TM.28z or control FMC63 CAR T cells on day 4 via IV tail vein injection. Tumor burden and weight was followed until the endpoint on day 18. **B)** weight of treated mice shown as change to baseline over the course of the experiment (mean \pm SEM) **C)** FLUX [P/s] values of tumor burden assessed by IVIS imaging (mean \pm SEM) and **D)** bioluminescence images **E)** Assessment of blood cell populations and liver function parameters (transaminases AST, ALT and alkaline phosphatase). Values represent mean \pm SD. Statistic represents Student's t-test (**** = $p < 0.0001$, *** = $p < 0.001$, ** = $p < 0.01$, * = $p < 0.05$, ns = $p > 0.05$). **F)** Hematoxylin and eosin [H&E] stained tissues from mice either treated with GPC2.19 28TM.28z CAR T cells (A-U images) or FMC63 control CAR T cells (A'-U' images). All tissues are histologically within normal limits, including heart (A, A'), lung (B, B'), liver (C, C'), spleen (D, D'), kidney (E, E'), esophagus (F, F'), trachea (G, G'), cerebrum (H, H'), stomach (I, I'), small intestine (J, J'), large intestine (K, K'), testes (L, L'), thyroid gland (M, M'), salivary gland (N, N'), cerebellum (O, O'), retina (P, P'), pancreas (Q, Q'), haired skin (R, R'), seminal vesicle (S, S'), brown adipose tissue (T, T') and white adipose tissue (U, U'). Magnification: 40x.